International Journal of Biological Macromolecules 139 (2019) 75–84

Contents lists available at ScienceDirect

International Journal of Biological Macromolecules

journal homepage: http://www.elsevier.com/locate/ijbiomac

Binding interactions of a series of sulfonated water-soluble resorcinarenes with bovine liver catalase

Nicole Collazos [a], Germán García [a], Andrés Malagón [a,*], Obradith Caicedo [b], Edgar F. Vargas [c]

[a] Departamento de Bioquímica, Facultad de Ciencias, Universidad Antonio Nariño, sede circunvalar, Colombia
[b] Departamento de Ciencias Básicas, Universidad Santo Tomás, Carrera 9 # 51-11, Bogotá, Colombia
[c] Departamento de Química, Universidad de Los Andes, Cra 1 N° 18A – 12, Colombia

ARTICLE INFO

Article history:
Received 14 June 2019
Received in revised form 24 July 2019
Accepted 29 July 2019
Available online 29 July 2019

Keywords:
Catalase
Enzyme
Resorcinarenes
Binding

ABSTRACT

Resorcinarenes are macrocyclic molecules that can bind different molecules in a supramolecular fashion. There are some sulfonated water-soluble derivatives that have been investigated to bind proteins avoiding fibrillation. The interaction with enzymes such as catalase (CAT) allows the interpretation of the possible effects of the use of resorcinarenes on human health or environmental applications. The interaction of five sulfonated resorcinarenes with different chemical structures was investigated by using different biophysical methods. The results of the spectroscopic experiments (fluorescence, synchronous fluorescence, and Uv-vis spectrophotometry) show different degrees of structural change, indicating that the binding of the macrocycles that were studied causes alterations on the conformation of CAT. The resorcinarenes reduce the activity of CAT in different extent, two macrocycles (named Na_4EtRA and Na_4PrRA, according to ethyl or propyl moieties at the lower pendant group) exhibit significant inhibition capacity (until ca. 70%). The study about inhibition types reveals a non-competitive mechanism for all the studied resorcinarenes. The docking calculations reveal that the macrocycles bond mainly to two domains of the CAT structure, which are not related with the active site.

1. Introduction

Bovine liver catalase (CAT) is a metalloenzyme that contains a heme prostetic group; the structure has four identical polypeptide chains. The catalytic action reduces hydrogen peroxide using the ferric ion by catalyzing its decomposition into molecular oxygen and water without the production of free radicals [1]. A relevant issue regarding the CAT activity is that the enzyme exhibits a high rate (over 40 million substrate molecules per second) and does not have a typical Michelis-Menten behavior, in formal terms, it does not reach saturation, but its kinetic behavior is described as a first order process [2].

Catalases are enzymes that play a crucial role on aerobic organisms, acting as protective agents against oxidative stress and playing a crucial role in the adaptive response to H_2O_2 [3]. Most catalases remain active in a great variety of pH and temperature conditions. Therefore, these enzymes can be used in industrial processes such as waste water treatment (mainly from the bleaching of textile fibers where hydrogen peroxide is extensively used), pharmacology, biosensors, biocatalysis, and foods [4]. The development of heterogeneous processes including catalases have allowed their use in environmental applications [5] and certain materials has been used as supports [6,7], namely to generate sensors of hydrogen peroxide in wastewater. In addition, the catalases have been used to detect water pollutants such as tetrabromobisphenol A (TBBPA) [8], or mercury [9]. The activity of catalases has been recognized as a biomarker of oxidative stress [10], and the role of enzymes to check pollution of xenobiotics has been confirmed [11–13] enzymatic tests are useful for the identification of toxicophore structures and to reduce potential toxicological effects of new molecules [14].

The resorcinarenes are macrocyclic molecules that form with the crown ethers, cyclodextrins and calixarenes, the main organic host compounds [15]. They can be obtained from the condensation of resorcinol and a suitable aldehyde yielding mostly tetrameric units in which the aromatic moieties are linked together by a methylene bridge. The aldehyde that is used in the synthesis provides a *tail* to the main cyclic structure allowing systematic modifications and, consequently, slightly modifying their reactivity [16]. Despite possible applications in biological and environmental fields, the basic cyclic structure is poorly water soluble. Therefore, the sulfonation is a good option to improve water solubility [17]. Some studies have been carried out to identify the binding between sulfonated resorcinarenes and amino acids or peptides [18].

The resorcinarenes can bind guests in a supramolecular fashion, due to their capacity to offer different intermolecular interactions because of their semi-rigid cone-shaped structure, the rich π-electron cavity, and the hydrogen binding sites [19]. The utility of resorcinarenes in

* Corresponding author.
E-mail address: edmalagon@uan.edu.co (A. Malagón).

https://doi.org/10.1016/j.ijbiomac.2019.07.197
0141-8130/

biological applications includes: the recognition of amino acids [20], a delivery tool in pharmacology [21], or recently, the ability to inhibit fibrillation of Aβ-amyloid [22]. The possibility to bind proteins generates promising pharmaceutical applications, since fibrillation is the cause of various illnesses known as amyloidosis.

In this work, we have employed spectroscopic methods, enzyme activity tests, and molecular docking to investigate the interaction of five water-soluble sulfonated resorcinarenes with CAT. The results that were obtained are discussed in terms of the influence of binding on the structure and enzyme activity changes. This study can contribute to clarify the possible toxicity of resorcinarenes and the influence of their binding on oxidative stress based on a potential use of resorcinarenes in pharmacology. In addition, it provides valuable information about the use of macrocyclic molecules on biological applications.

2. Materials and methods

2.1. Chemicals

Bovine liver catalase (CAT, 2000–5000 U/mg) was purchased from Sigma (USA). Hydrogen peroxide (30%), sodium hydrogen phosphate (>99.0%) and disodium hydrogen phosphate (>98.0%) were purchased from PanReac (USA). The phosphate buffer (50 mM, pH 7,4) was used in all experiments, pH measurements were made with a Hand-held pHmeter (Boeco, Germany). The ultrapure water to prepare the solutions was obtained using a MilliQ system (conductivity >18 MΩcm).

2.1.1. Resorcin[4]arenes

Sodium *c*-methylsulfonateresorcin[4]arene (Na_4MeRA), c-ethylsulfonateresorcin[4]arene (Na_4EtRA), c-propylsulfonateresorcin [4]arene (Na_4PrRA), c-methytioethylsulfonateresorcin[4]arene (Na_4SRA), and c-esulfonateresorcin[4]arene (Na_4ESRA), were synthetized according to procedures reported in literature [23]. The purity of these compounds was better to 98%. Fig. 1 shows the molecular structure of the resorcin[4]arenes used. All macrocycles show the cone conformation.

2.2. Determination of the CAT activity

To determine the best conditions to test the CAT activity, an experimental design 2^2 at pH 7.4 was used, testing enzyme and substrate concentrations. The CAT activity was measured using a Cary 60 spectrophotometer (Agilent, USA), by detecting the hydrogen peroxide decomposition at 240 nm (A_{240}), measured every 3 s for 30 s at 298.15 K [2]. The CAT concentrations were evaluated in the range of 1.0 to 10.0 μM and H_2O_2 from 1.8 to 18.0 μM. And the temperature was maintained at 298.15 K.

The effect of the resorcinarenes on the activity of CAT was determined as a function of H_2O_2 concentration (5.0–50.0 μM) in the presence of 0, 10.0, 20.0, 50.0, and 100.0 μM of the target resorcinarene. The enzyme concentration in all assays was 10 μM, and the substrate concentration was 18 μM (as resulted from the best conditions). Since within time the absorbance was linear at 240 nm, we used the slope of the straight line to define the CAT activity along with the relative rate of enzyme reactions. The activity data for all studied systems were expressed as relative activity using the results of a blank control as 100% (that is, the reaction in absence of resorcinarene). The values were presented as means ± standard error of the mean (SD) of three independent experiments. Multiple comparisons among experiments containing resorcinarenes and control groups were assessed using ANOVA and Tukey's test.

To test the inhibition type, the enzyme concentration was maintained at 10 μM, and the resorcinarene concentrations were: 0,10, 20 50, and 100 μM; while the substrate concentrations were: 0, 5, 8, 14, 25, and 50 μM.

2.3. UV–vis absorption measurements.

The Uv-vis spectra were measured using a Cary 60 spectrophotometer (Agilent, UAS) in the wavelength range of 200 to 700 nm. A quartz cuvette of 1 cm path length equipped with a Peltier system to control the temperature was used. The CAT concentration was constant at 1.0 μM and the resorcinarenes ranged from 0 to 20.0 μM. All measurements were performed allowing 3 min of incubation to ensure thermal equilibrium at 298.15 K.

2.4. Fluorescence and synchronous fluorescence experiments.

The fluorescence spectra were recorded using a Cary Eclipse spectrophotometer (Agilent, USA) equipped with a quartz cuvette of 1 cm path length. In the experiments the excitation and the emission slit widths were set at 5.0 nm, the scan speed was 1200 nm/min, and the photo multiplier voltage was fixed to 600 V. The excitation wavelength was 280 nm and the emission spectra were recorded from 300 to 500 nm. The inner filter effect (IFE) caused by the absorption during excitation and emission processes were corrected using Eq. (1) [24].

$$F_{cor} = F_{obs}\, x\, 10^{\frac{A_1 + A_2}{2}} \quad (1)$$

where F_{cor} and F_{obs} correspond to the corrected and observed fluorescence, respectively. $A_1$and A_2 are the absorbances at the excitation and maximum emission wavelengths, respectively.

For the synchronous measurements the spectra were measured using a fixed wavelength interval between the excitation and emission wavelengths (Δλ = 15 nm and 60 nm), and the excitation wavelength

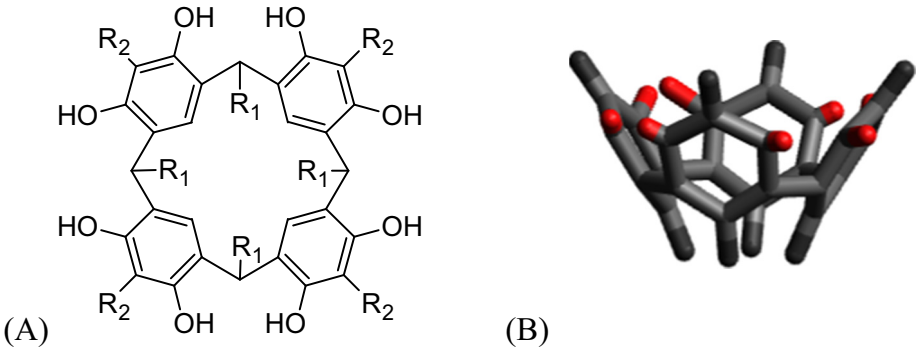

Fig. 1. A. The molecular structures of Resorcinarenes used in this work. Na_4MeRA R_1 = –CH_3, R_2 = CH_2SO_3Na; Na_4EtRA R_1 = –CH_2CH_3, R_2 = CH_2SO_3Na; Na_4PrRA R_1 = - CH_2 CH_2CH_3, R_2 = CH_2SO_3Na; Na_4SRA R_1 = - CH_2 CH_2SCH_3, R_2 = CH_2SO_3Na; Na_4ESRA R_1 = - $CH_2CH_2SO_3Na$, R_2 = H. B. Cone conformation of the resorcinarenes.

was recorded from 250 to 320 nm. In all fluorescence experiment the CAT concentration was maintained at 2.0 μM and the resorcinarenes ranged from 0 to 40.0 μM. The solutions were maintained three minutes at 298.15 K.

2.5. Molecular docking study

The interaction between CAT and the target resorcinarenes was explored Swiss Dock server [25]. The structures of all resorcinarenes were optimized by using the gaussian method on the Avogadro software [26]. The docking follows a blind method in which the entire protein is selected; since all four chains of CAT are similar, only chain A was selected for the theoretical studies. The crystal structure of bovine liver CAT (PDB code: 1TGU) was downloaded from the RCSB Protein Data Bank (http://www.pdb.org/). The docking results were screened by Chimera [27].

3. Results and discussion

3.1. Effect of resorcinarenes on the catalase activity

The activity of enzymes is closely related to the structure, any change on structure may lead to loss of activity or complete inactivation. The effect of the five studied resorcinarenes on the activity of CAT was

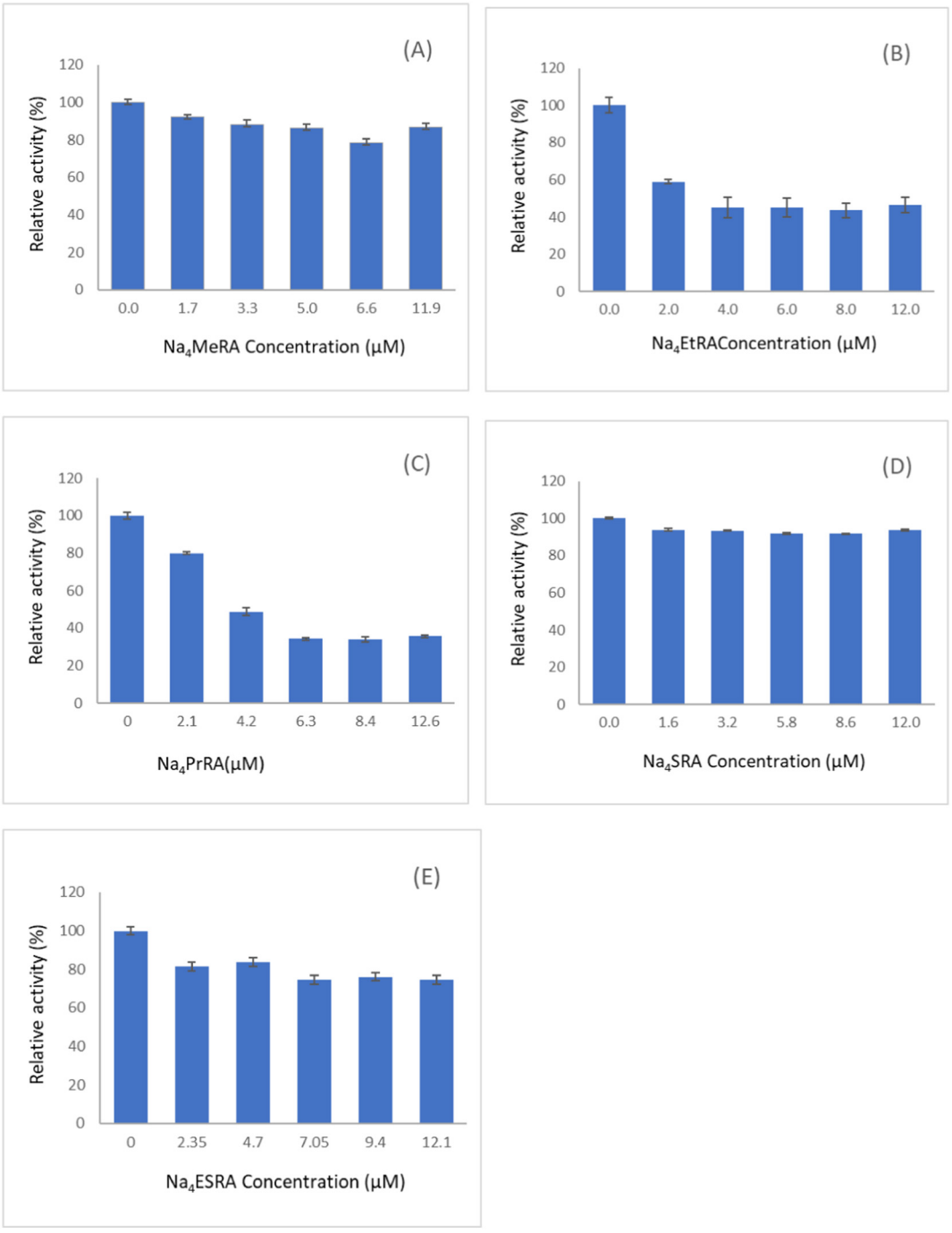

Fig. 2. Changes in the CAT activity in presence of different concentration of resorcinarenes. (A) Na_4MeRA, (B) Na_4EtRA, (C) Na_4PrRA, (D) Na_4ESRA, (E) Na_4SRA. Values are means ± SD ($n = 3$).

followed and the results are shown in Fig. 2. These results show an effect of inhibition on the CAT activity due to the presence of macrocycles. This effect can be represented by the following tendency: **Na_4PrRA** > **Na_4EtRA** > **Na_4ESRA** > **Na_4MeRA** > **Na_4SRA**.

The inhibitory effect of the resorcinarenes on the CAT enzyme can occur in various ways. There are three types of inhibition: competitive, uncompetitive, and non-competitive [28]. To obtain information about the inhibition mechanism, the Lineweaver-Burk plots were used, they are show in Fig. 3. This is a useful method to estimate the inhibition mechanism based in a simple double-reciprocal plot, in which the Michaelis constant and the maximum velocity can be inferred from the intercept and the slope of the obtained plot. It was observed that for all studied systems, the slope of the plots increases with the increase of resorcinarene concentration and their fitted lines converged on the x-axis. This behavior is related mainly with a non-competitive type of inhibition [28,29]. This type of inhibition has been observed with other inhibitors such as: chrysoidine [28] and 6-benzylaminopurine [30] which are characterized by the presence of aromatic moieties in their structures. The mechanism surrounding a non-competitive inhibition consists in a bind of the macrocycle to the enzyme where the substrate does not bind, either the free enzyme or the enzyme-substrate complex, in any case, the enzyme-substrate-inhibitor complex is not formed.

3.2. The effect of resorcinarenes on the fluorescence spectra of CAT

The aromatic amino acid residues contribute to the intrinsic fluorescence of CAT, tryptophan (Trp), tyrosine (Tyr), and phenylalanine (Phe). At 298 nm excitation wavelength, the emission fluorescence is dominated by Trp and Tyr, and is very sensitive to the microenvironment of these residues [30]. The changes in the intensity and spectral characteristics of Trp and Tyr can also be attributed to their exposure to the solvent as well as on interaction with other amino acids and groups like heme, etc. [31]. In addition, the changes in the fluorescence spectrum of CAT can be used to study the quenching mechanism and to obtain binding constants [30,32].

Fig. 4 shows the fluorescence spectra of the interaction of CAT with resorcinarenes. The results show that the fluorescence intensity of CAT decrease when resorcinarene concentration increases, following the tendency **Na4ESRA** > **Na_4SRA** > **Na_4EtRA** > **Na_4MeRA**. The exception to this behavior is **Na_4PrRA**, which increase the fluorescence intensity with the increase of concentration. In addition, these results indicate an association CAT-resorcinarene that alter the microenvironment around the fluorophore residues of the enzyme.

To obtain information on the nature of the interaction between CAT and the resorcinarenes, when the macrocycles act as quenchers (that is,

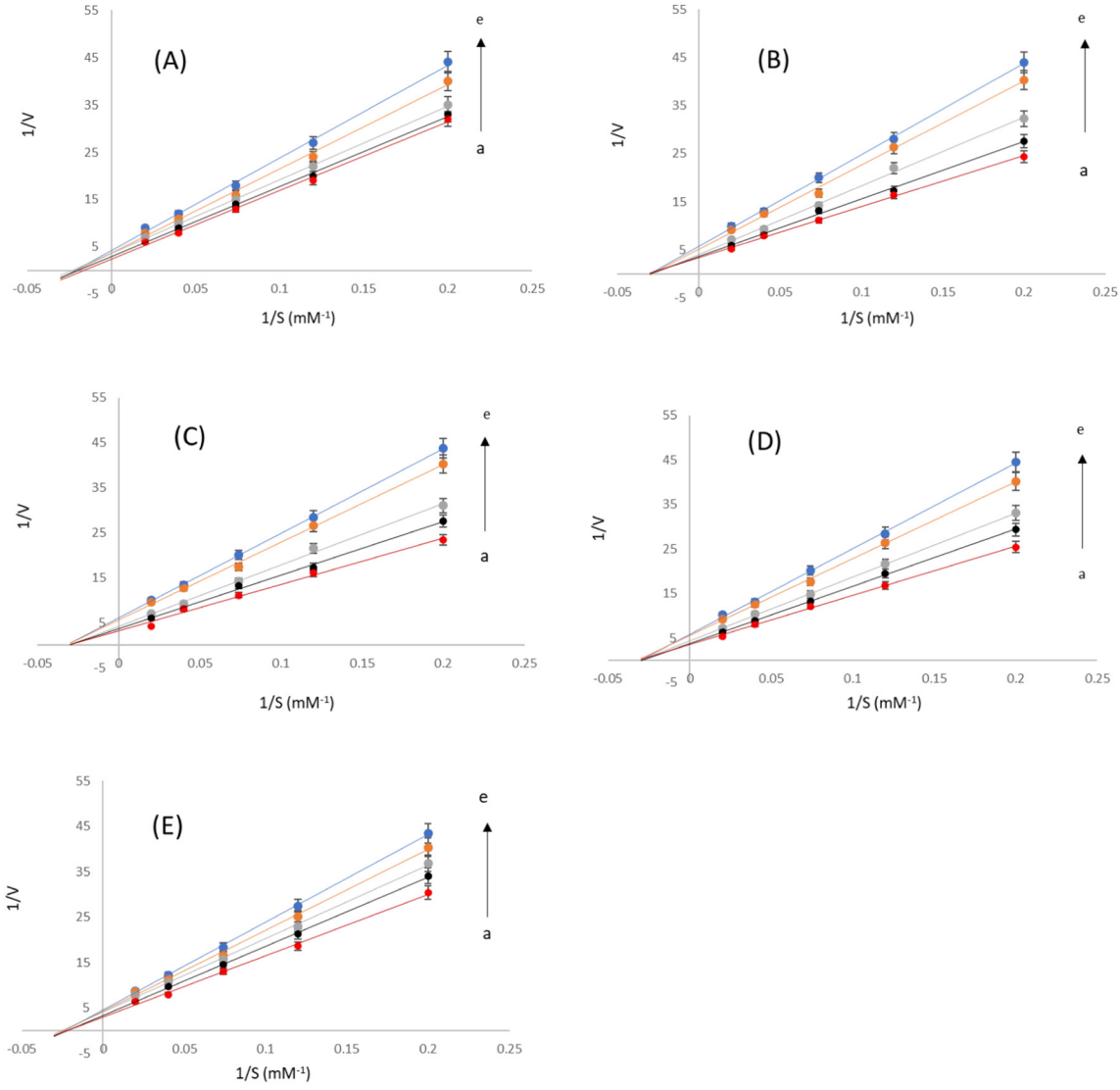

Fig. 3. Lineweaver–Burk plots for inhibition of the CAT activity in the absence and presence of (A) Na_4MeRA, (B) Na_4EtRA, (C) Na_4PrRA, (D) Na_4ESRA, and (E) Na_4SRA. The data points and error bars indicate the mean ± SEM of three repetitions, at different concentrations of resorcinarene: (μM a-k) 50, 25, 14, 8, and 5.

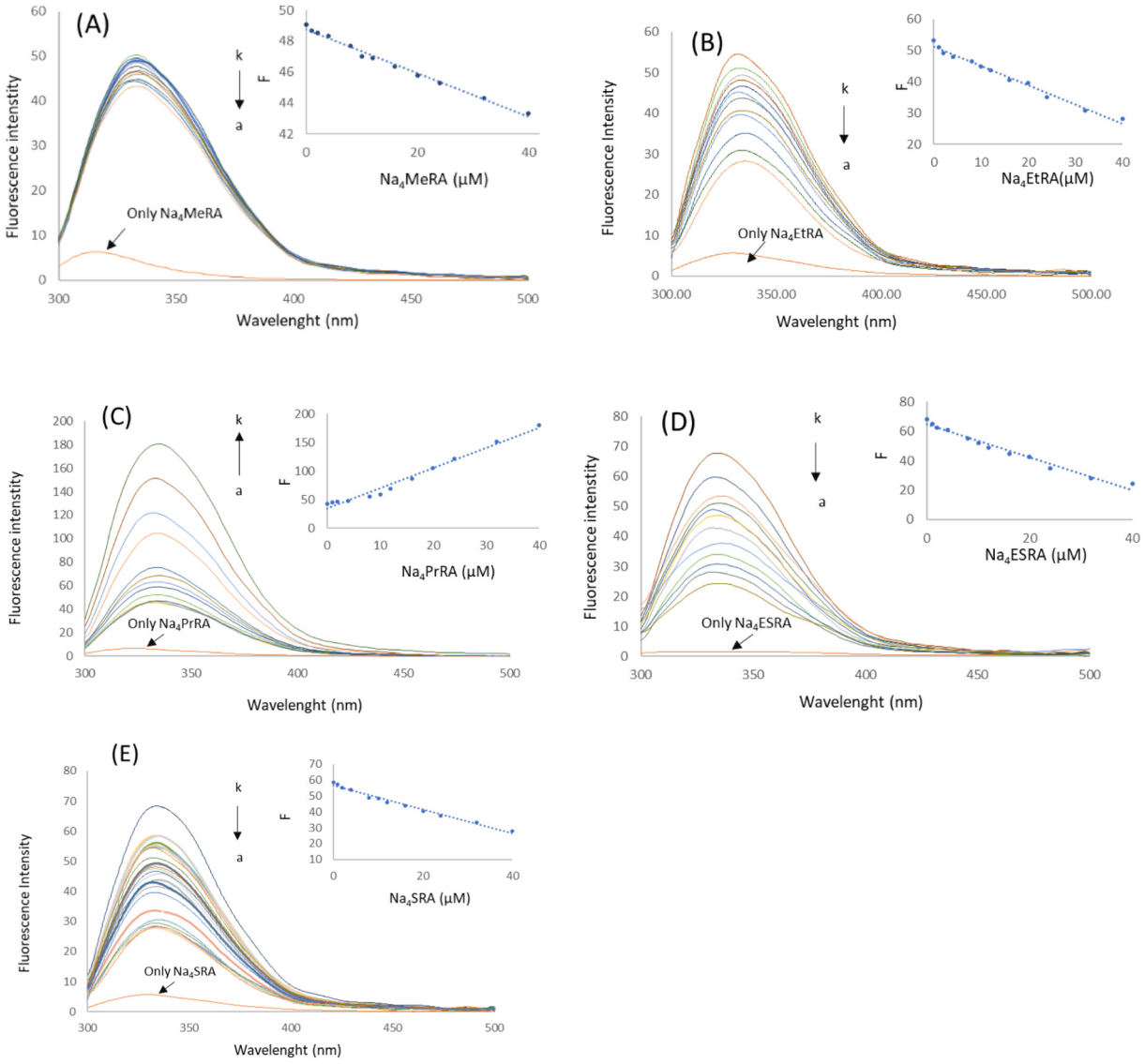

Fig. 4. The fluorescence spectra of CAT in the presence of (A) Na_4MeRA, (B) Na_4EtRA, (C) Na_4PrRA, (D) Na_4ESRA, and (E) Na_4SRA. The insets are the scatter plots of fluorescence intensity at different concentrations of resorcinarene: (μM a-k) 0.5, 1.0, 2.0, 8.0, 10.0, 12.0, 16.0, 20.0, 24.0, 32.0, and 40.0.

Na4ESRA, Na_4SRA, Na_4EtRA, Na_4MeRA), the Stern-Volmer quenching constant was calculated using Eq. (2) [33–35].

$$\frac{F_0}{F} = 1 + K_{sv}[Q] = 1 + K_q\tau_0[Q] \quad (2)$$

whereas, the accessibility of the tryptophan residues to the macrocycles was tested using Eq. (3) [36].

$$log\left(\frac{(F_0 - F)}{F}\right) = \log K_A + n log[Q] \quad (3)$$

In Eqs. (2) and (3), K_{sv} is the Stern-Volmer quenching constant, K_q is the quenching rate constant of the enzyme, and τ_0 is the fluorescence lifetime in the absence of quencher, which is 10^{-8} s for CAT [37] F_0 and F are the fluorescence intensities of CAT in the absence or presence of quencher (Resorcinarene), [Q] is the total concentration of resorcinarene, K_A is the binding constant, and n is the Hill's coefficient related to the number of binding sites. The values that were obtained are listed in Table 1.

Regarding the quencher resorcinarenes, the procedures described in Eq. (1) and (2) were applied. The linearity of Eq. (2) has been related with the dominance of binding mechanism [30,38]. In this way, the results show that the Stern-Volmer model is appropriate to study the interaction CAT-resorcinarene. In addition, the values of the typical K_q values of quenchers have been obtained as 2.0×10^{10} M^{-1} s^{-1}, for all

Table 1
Values of K_{sv}, K_q , K_A, and n for the interaction of quenchers and CAT.

Quencher	$10^6 \cdot K_{sv}$ ($dm^3 \cdot mol^{-1}$)	$10^{13} \cdot K_q$ ($dm^3 \cdot mol^{-1} \cdot s^{-1}$)	R^2 (Eq. (2))	S.D. (Eq. (2))	$10^5 \cdot K_A$ (M^{-1})	n	R^2 (Eq. (3))	S.D. (Eq. (3))
Na_4MeRA	3.2	32	0.99	0.02	6.05	2.1	0.98	0.01
Na_4EtRA	21.8	218	0.98	0.03	6.12	1.4	0.95	0.02
Na_4EsRA	26.1	261	0.98	0.03	9.83	1.7	0.99	0.02
Na_4SRA	45.1	451	0.97	0.03	8.89	1.4	0.97	0.03

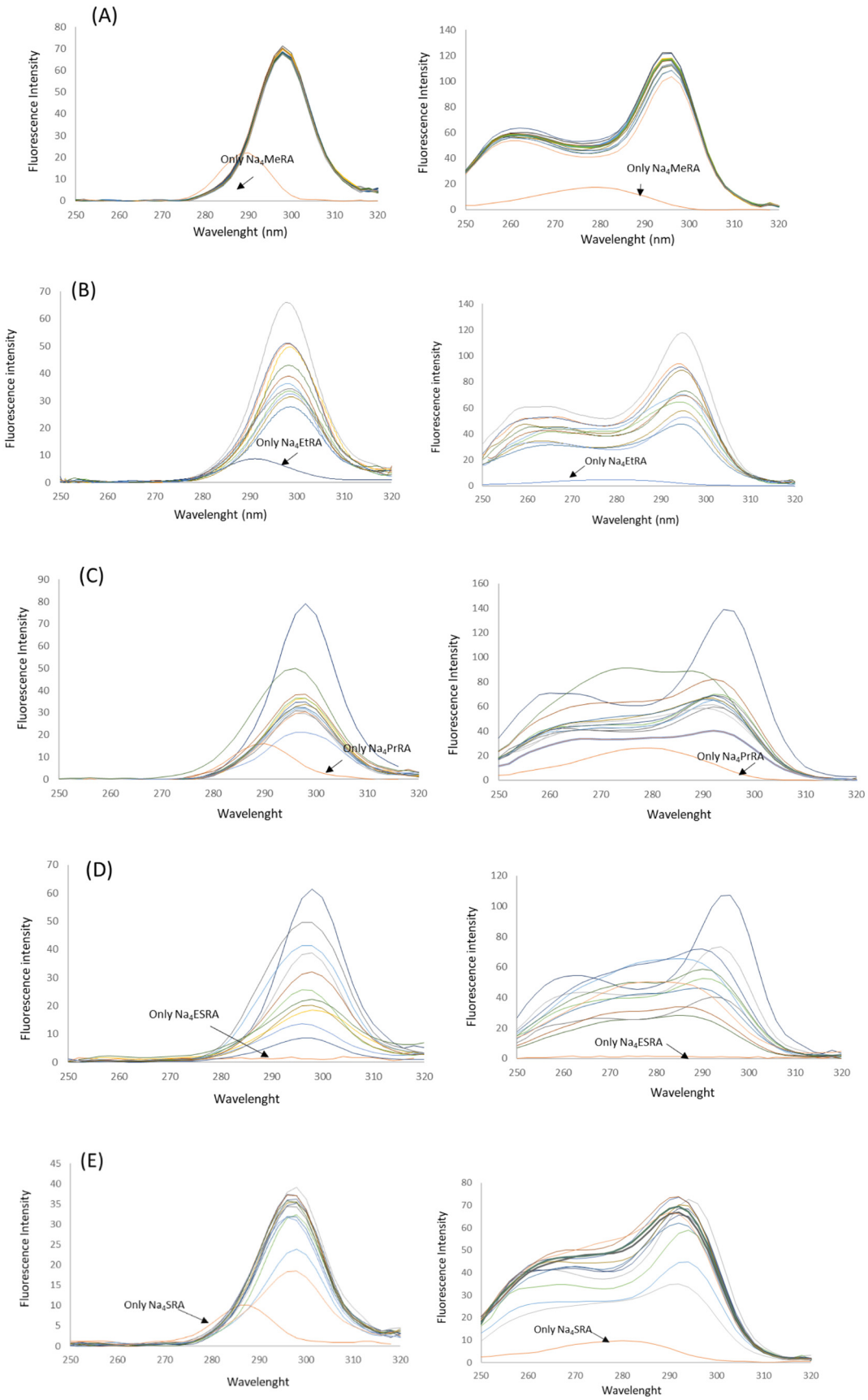

Fig. 5. Synchronous fluorescence spectra of (A) Na_4MeRA, (B) Na_4EtRA, (C) Na_4PrRA, (D) Na_4ESRA, and (E) Na_4SRA with CAT. $\Delta\lambda = 15$ nm (right side), and $\Delta\lambda = 60$ nm (left side). Experimental conditions: (resorcinarene μM a-k) 0.5, 1.0, 2.0, 8.0, 10.0, 12.0, 16.0, 20.0, 24.0, 32.0, 40.0.

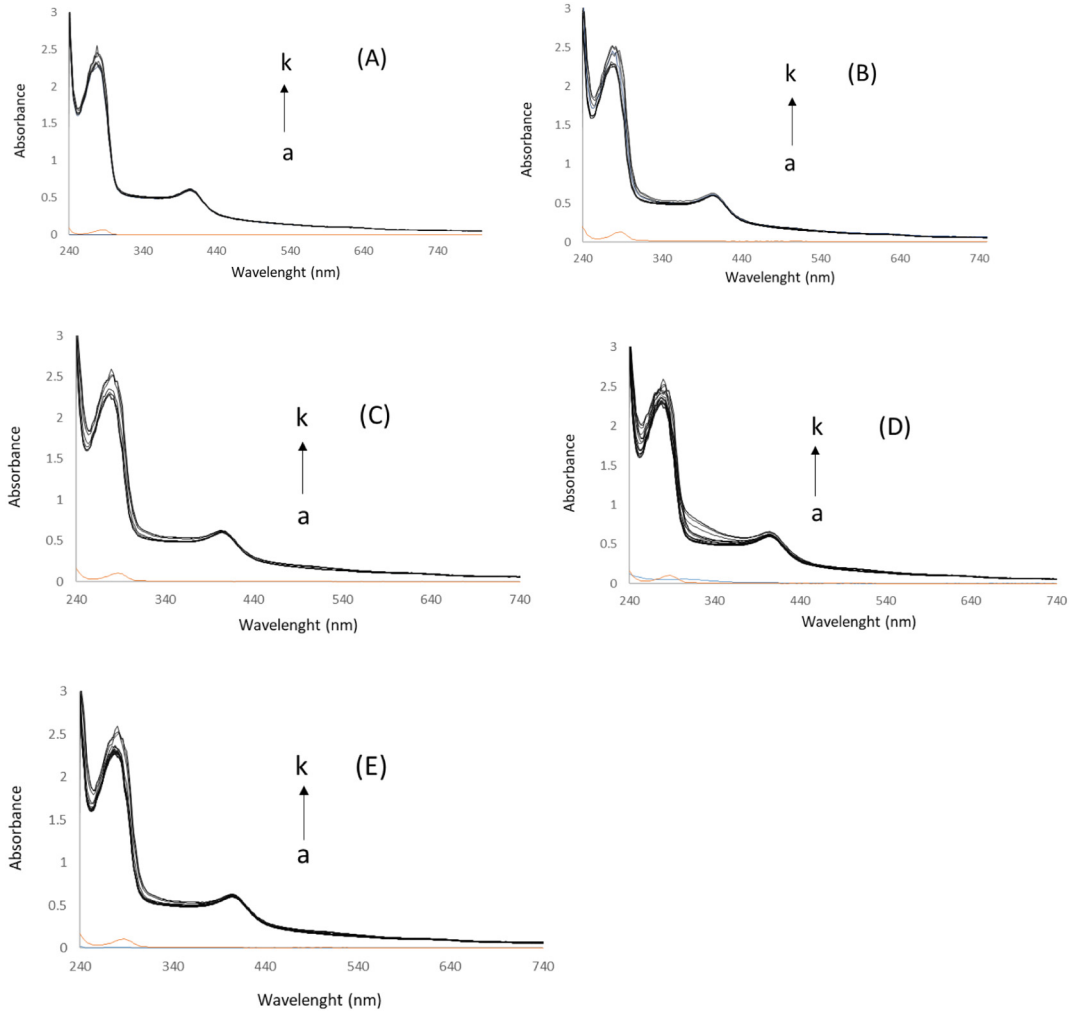

Fig. 6. UV–vis absorption spectra of CAT in the absence and presence of (A) Na_4MeRA, (B) Na_4EtRA, (C) Na_4PrRA, (D) Na_4ESRA, and (E) Na_4SRA. Experimental conditions: (resorcinarene μM a-k) 0.5, 1.0, 2.0, 8.0, 10.0, 12.0, 16.0, 20.0, 24.0, 32.0, 40.0.

studied quenching resorcinarenes the K_q obtained values are larger, which shows that the static mechanism is predominant [37,39].

Considering that the fluorescence quenching is associated with binding, the values of the respective binding constants (K_A) and the number of n binging sites were calculated using Eq. (3) and the results are shown in Table 1. The n values that were obtained indicate the existence of 1 or 2 binding sites. On the other hand, the affinity defined by K_A indicate a strong interaction CAT-resorcinarene, following the tendency: Na_4ESRA > Na_4SRA > Na_4EtRA > Na_4MeRA. The obtained values are similar to those obtained for other quenchers such as flavonoids [31] and farnesiferol [34,] which also show a strong interaction with the CAT enzyme.

In this work, an enhancement of fluorescence intensity is observed in the interaction of CAT with Na_4PrRA, it would be reasonable to hypothesize that the enhancement of fluorescence is due to a complexation with CAT in a different fashion observed for the other macrocycles. The fluorescence signal is strongly influenced by the environment around the molecule, on the other hand, potential effects of the formation of a strong fluorescent complex could be considered.

3.3. Synchronous fluorescence studies

The synchronous fluorescence spectra are used to provide information on the molecular environment in the vicinity of the CAT fluorophore groups (mainly Trp and Tyr). In this study two D-values (Δλ) at 15 or 60 nm were determined and are reported in Fig. 5.

The exposition of Trp and Tyr residues to the solvent, because of the interaction with the ligands, is associated with a red shift in the emission maxima, whereas a blue shift can be noticed in an opposite situation. The synchronous fluorescence intensity was measured for the five resorcinarenes using the same concentration range for all ligands. A significant change in the maximum emission wavelength is not

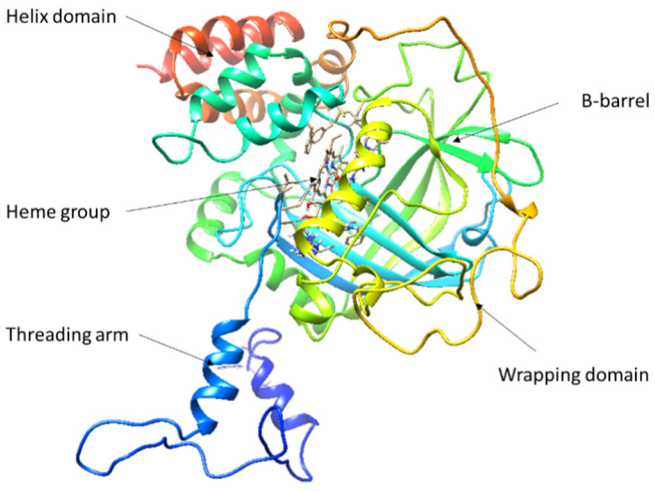

Fig. 7. The structure of CAT (the conformational domains are highlighted).

Table 2
Obtained binding sites, residues and distance to heme group.

Resorcinarene	Domain	Binding residues	Distance to iron in heme group (Å)
Na_4MeRA	Wrapping domain	Arg 65, Ile 372, Pro 373, Met 391, Met 393.	13.7
Na_4EtRA	β-barrel	Leu 158, Gln 351, Gly 352, Leu 354, Phe 355, Arg 430	11.0
Na_4PrRA	β-barrel	Lys 348, Arg 353, Leu 354, Arg 430	10.6
Na_4SRA	β-barrel, Wrapping domain	Leu 158, Lys 348, Gly 352, Phe 355, Phe 431	12.4
Na_4ESRA	β-barrel, Wrapping domain	Asp 427, Gln 429, Arg 430, Phe 431	16.0

noticeable in Na_4MeRA, Na_4EtRA and Na_4SRA. Nevertheless, a remarkable change is observed in the Na_4PrRA, and Na_4ESRA spectra. These results indicate significant effects on the microenvironment of Trp and Tyr residues during the binding process with Na_4PrRA and Na_4ESRA [35].

3.4. Uv-Vis spectrophotometric studies

The Uv-vis absorption spectrometry is useful to explore possible structural changes in the protein due to the binding with ligands. In the case of CAT, two main bands offer important information, the first one at 280 nm, that is attributed to aromatic aminoacids (Tyr, Trp, and Phe), and the second one at 405 nm that is known as the Soret band due to the absorption of the heme group [40]. The obtained Uv-vis spectra are shown in Fig. 6.

No changes in the absorption maxima are produced due to the addition of resorcinarenes. However, the absorption peaks at 280 show some increment compared to the native enzyme. The Na_4MeRA and Na_4ESRA has the least significant changes. It may be concluded that all resorcinarenes bind CAT by means of changing the protein conformation and causing little effect on the heme group.

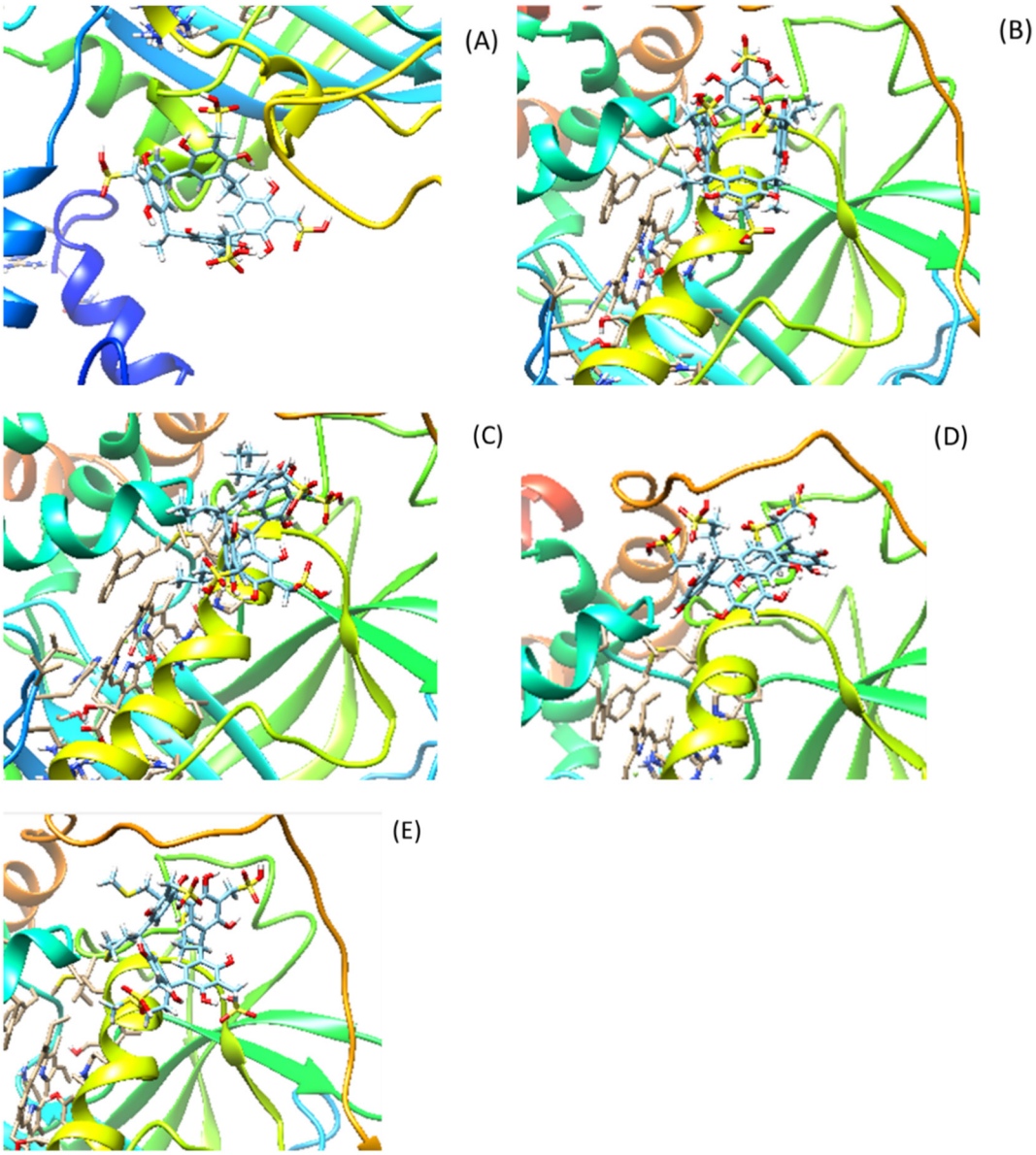

Fig. 8. Structures of the resorcinarenes docked in a catalase monomer. (A) Na_4MeRA, (B) Na_4EtRA, (C) Na_4PrRA, (D) Na_4ESRA, and (E) Na_4SRA.

3.5. Computational modeling of the resorcinarene-CAT complexes

Molecular docking studies were performed to simulate possible binding sites between the studied resorcinarenes and CAT. The docking studies are commonly used to clarify the mechanism of structural and activity changes. The CAT enzyme is a tetrameric protein in which all subunits are identical. One subunit of the tetrameric enzyme (Chain A) was selected to obtain the docking studies, each subunit is composed of a single polypeptidic chain of 527 residues. The Swiss dock program that was used in this study allows a calculation in which is not necessary to limit any region in the protein, the entire chain is considered (blind docking). Each chain conforming CAT can be described as composed by domains: helix domain, β-barrel, wrapping domain, and threading arm (as described in Fig. 7). The active-center region of catalase contains a heme molecule bonded to an unprotonated tyrosine residue (Tyr343), which in turn is hydrogen bonded to a conserved arginine residue (Arg339). On the distal side, two polar residues (His61 and Asn133) and two nonpolar residues (Phe138 and Phe146) enclose the active site [41].

Docking results revealed that each resorcinarene has a preferential binding site. The description of all obtained binding sites is shown in Table 2. In addition, Fig. 8 indicates the binding of each studied resorcinarene on the CAT structure. The binding sites that were obtained were chosen considering the lower energy values obtained for all clusters.

Two main domains on the CAT structure provide binding sites: the cavity in the middle of the β-barrel and the wrapping domain (as described on Fig. 7). On the other hand, the resorcinarenes are oriented in a regular fashion: the upper rim (where the sulfonated residues are located) oriented oppositing the polypeptydic sequence, and the lower rim (where the hydrophobic chain is located) oriented facing the protein. The detailed computational results indicate main hydrophobic interactions and van der Waals forces.

The docking results can be correlated with the results that were obtained from the fluorescence quenching analysis that were discussed earlier. According to fluorescence experiments no quenching is noticed for Na_4PrRA, and the possible binding residues obtained from docking calculations do not include any aromatic residue. Another feature about the binding of Na_4PrRA is that the resorcinarene also contains the longer hydrophobic pending tail, allowing a deeper introduction into the β-barrel subunit, disturbing the structure of the hydrophobic environment around the catalytic site described earlier.

According to docking results, no direct interaction has been found between the studied resorcinarenes and the residues related to enzyme activity (His 61, Asn 133, Phe 138, Phe146, Arg 339 and Tyr 343) or the heme group. Additionally, the heme group is buried under the protein structure, and the binding sites of Na_4PrRA and Na_4EtRA are the closer to the active site of CAT (the distances reported in Table 2 are obtained from the iron atom and the ligand), besides Na_4PrRA and Na_4EtRA also have the closer interaction with catalytic site. So, the binding interaction between Na_4PrRA and Na_4EtRA could cause indirect structural changes in both the catalytic site and could also affect the enzyme activity in a higher degree. These results agree with the Uv-vis spectra that shows little interaction with the heme group. In addition, the fluorescence experiments also agree showing enhancement of the fluorescence in the interaction between CAT and Na_4PrRA, where no interaction with aromatic residues are noticed, in contrast to the other macrocycles that were tried.

In addition, the docking calculation evidences several possible binding sites, in this work, we offer many options (see Table 2). Considering that the fluorescence experiments can be related to 1 or 2 sites. However, none of them implies a competitive inhibition type. A direct relationship between distances heme-resorcinarene and changes in activity cannot be addressed. It seems reasonable that the docking results are enough to propose binding sites and explain main results regarding activity of CAT towards the studied resorcinarenes. The results that were obtained from the docking calculations agree with the ones obtained from the non-competitive inhibition type discussed earlier.

The substrate channel has been described previously and the heme site is accessible through an array with polar and non-polar residues located at the β-barrel domain [42]. According to docking calculations, the stronger inhibitors (Na_4EtRA and Na_4PrRA) only can bind this domain, suggesting that the inhibitory effect can be explained as an obstruction of the substrate channel.

4. Conclusions

In this work, the influence of the binding of a series of water soluble resorcinarenes (Na_4MeRA, Na_4EtRA, Na_4PrRA, Na_4SRA, and Na_4ESRA) with CAT is explored by spectroscopic methods, enzyme activity measurements, and molecular docking calculations. The microenvironment and conformation of CAT were altered as a consequence of the binding that can be addressed from fluorescence, synchronous fluorescence, and Uv-vis spectra. Results showed a conformational change following the tendency: Na_4MeRA > Na_4EtRA > Na_4SRA > Na_4ESRA, and an enhancement of fluorescence emission in the presence of Na_4PrRA. All resorcinarenes diminish CAT enzyme activity, following the tendency: Na_4SRA > Na_4MeRA > Na_4ESRA > Na_4EtRA > Na_4PrRA. According to the docking results, no resorcinarene can bind directly to the heme group, or the residues implied in the CAT activity, but the substrate channel can be affected. The structural changes cannot be directly correlated to enzyme activity. However, the binding of the macrocycles that have been studied can be related to the proximity to the active site and the binding to two sites of CAT: the β-barrel and the wrapping domain. This study provides experimental evidence for the better understanding of the interaction of sulphonated resorcinarenes with proteins and the possible toxicity of resorcinarenes in the interest of using it in environmental and pharmaceutical applications.

Acknowledgments

Authors acknowledge to financial support from Universidad Antonio Nariño (project 2017222), Universidad de los Andes (Facultad de Ciencias), and FODEIN-Universidad Santo Tomás.

References

[1] J. Vlasits, C. Jakopitsch, M. Bernroitner, M. Zamocky, P.G. Furtmüller, C. Obinger, Mechanisms of catalase activity of heme peroxidases, Arch. Biochem. Biophys. 500 (2010) 74–81.
[2] H. Aebi, Methods in Enzymology, vol. 105, Academic Press. Inc, 1984 121–126 ISBN 0.12-182005-X105.
[3] H.S. Tehrani, A.A. Moosavi-Movahedi, Catalase and its mysteries, Prog. Biophys. Mol. Biol. 140 (2018) 5–12.
[4] N. Lončar, M.W. Fraaije, Catalases as biocatalysts in technical applications: current state and perspectives, 99 (8) (2015) 3351–3357.
[5] A.G. Grigoras, Catalase immobilization—a review, Biochem. Eng. J. 117 (2017) 1–20.
[6] A.M. Eberhardt, V. Pedroni, M. Volpe, M.L. Ferreira, Immobilization of catalase from *Aspergillus niger* on inorganic and biopolymeric supports for H_2O_2 decomposition, Appl. Catal. B 47 (2004) 153–163.
[7] J. Kaushal, S. Mehandia, G. Singh, G. Singh, S. Kumar, Catalase enzyme: application in bioremediation and food industry, Biocatal. Agric. Biotechnol. 16 (2018) 192–199.
[8] S. Dong, S. Wang, E. Gyimah, N. Zhu, K. Wang, X. Wu, Z. Zhang, A novel electrochemical inmunosensor based on catalase functionalized AuNPs-loaded self-assembled polymer nanospheres for ultrasensitive detection of tetrabromobisphenol A bis(2-hydroxyethyl)ether, Anal. Chim. Acta. 1048 (2019) 50–57.
[9] B. Elsebaia, M.E. Ghicab, M.N. Abbasa, C.M.A. Brett, Catalase based hydrogen peroxide biosensor for mercurydetermination by inhibition measurements, J. Hazard. Mater. 340 (2017) 344–350.
[10] S. Kourdali, A. Badis, A. Boucherit, Degradation of direct yellow 9 by electro-Fenton: process study and optimization and, monitoring of treated water toxicity using catalase, Ecotoxicol. Environ. Saf. 110 (2014) 110–120.
[11] H. Bártíková, L. Skálová, L. Stuchlíková, I. Vokrál, T. Vanek, R. Podlipna, Xenobiotic-metabolizing enzymes in plants and their role in uptake and biotransformation of veterinary drugs in the environment, Drug. Metab. Rev. Early Online (2015) 1–14.
[12] M. Dazy, J.F. Masfaraud, J.F. Férard, Induction of oxidative stress biomarkers associated with heavy metal stress in Fontinalis antipyretica Hedw, Chemosphere 75 (2009) 297–302.
[13] M. Solé, S. Rodríguez, V. Papiol, F. Maynou, J.E. Cartes, Xenobiotic metabolism markers in marine fish with different trophic strategies and their relationship to

ecological variables, Comp. Biochem. Physiol. C: Pharmacol. Toxicol. 149 (2009) 83–89.
[14] J. Arning, S. Stolte, A. Böschen, F. Stock, W.-R. Pitner, U. Welz-Biermann, B. Jastorffa, J. Ranke, Qualitative and quantitative structure activity relationships for the inhibitory effects of cationic head groups, functionalized side chains and anions of ionic liquids on acetylcholinesterase, Green Chem. 10 (2008) 47–58.
[15] H.J. Schneider, Mechanisms of molecular recognition: investigations of organic host-guest complexes, Angew. Chem. Int. Ed. Engl. 30 (1991) 1417–1436.
[16] P. Timmerman, W. Verboom, D.N. Reinhoudt, Resorcinarenes, Tetrahedron 52 (8) (1996) 2663–2704.
[17] E. Sanabria, M. Maldonado, M.A. Esteso, E.F. Vargas, Volumetric and acoustic properties of two sodium sulfonateresorcin[4]arenes in water and dimethylsulfoxide, J. Mol. Liq. 249 (2018) 868–876.
[18] L. Mutihac, H.-J. Buschmann, R.-C. Mutihac, E. Schollmeyer, Complexation and separation of amines, amino acids, and peptides by functionalized calix[n]arenes, J. Incl. Phenom. Macrocycl. Chem. 51 (2005) 1–10.
[19] H. Mansikkamki, M. Nissinen, K. Rissanen, Noncovalent π-π stacked exo-functional nanotubes: subtle control of resorcinarene self-assembly, Angew. Chem. Int. Ed. 43 (2004) 1243–1246.
[20] W.M. Hassen, C. Martelet, F. Davis, S.P.J. Higson, A. Abdelghani, S. Helali, N. Jaffrezic-Renault, Calix[4]arene based molecules for amino-acid detection, Sensors Actuators B Chem. 124 (2007) 38–45.
[21] B. Mokhtari, K. Pourabdollah, Applications of calixarene nano-baskets in pharmacology, J. Incl. Phenom. Macrocycl. Chem. 73 (2012) 1–15.
[22] X. Han, J. Park, W. Wu, A. Malagon, L. Wang, E. Vargas, A. Wikramanayake, K.N. Houk, R.M. Leblanc, A resorcinarene for inhibition of Aβ fibrillation. Chem. Sci. 8 (2017) 2003–2009, Tetrahedron Lett. 42 (51) (2000) 10111–10115.
[23] E. Kazakova, N. Makarova, A. Ziganshina, L. Muslinkina, A. Muslinkina, W. Habicherb, (Novel water-soluble tetrasulfonatomethylcalix[4]resorcinarenes).
[24] Z.X. Chi, R.T. Liu, T. Yue, X.Y. Fang, C.Z. Gao, Binding of oxytetracycline to bovine serum albumin: spectroscopic and molecular modeling investigations, J. Agric. Food Chem. 58 (2010) 10262–10269.
[25] A. Grosdidier, V. Zoete, O. Michielin, Swissdock a protein-small molecule docking web service based on EADock DSS, Nucleic Acids Res. 39 (2011) 270–277.
[26] M.D. Hanwell, D.E. Curtis, D.C. Lonie, T. Vandermeersch, E. Zurek, G.R. Hutchison, Avogadro: an advanced semantic chemical editor, visualization, and analysis platform, J. Chem. 4 (2012) 1–17.
[27] E.F. Pettersen, T.D. Goddard, C.C. Huang, G.S. Couch, D.M. Greenblatt, E.C. Meng, T.E. Ferrin, UCSF chimera—a visualization system for exploratory research and analysis, J. Comput. Chem. 25 (2004) 1605–1612.
[28] B. Yang, F. Hao, J. Li, D. Chen, R. Liu, Binding of chrysoidine to catalase: spectroscopy, isothermal titration calorimetry and molecular docking studies, J. Photochem. Photobiol. B 128 (2013) 35–42.
[29] S. Islamovic, B. Galic, M. Milos, A study of the inhibition of catalase by dipotassium trioxohydroxytetrafluorotriborate K2[B3O3F4OH], J. Enzyme Inhib. Med. Chem. 29 (5) (2014) 744–748.
[30] Q. Xu, Y. Lu, L. Jing, L. Cai, X. Zhu, J. Xie, X. Hu, Specific binding and inhibition of 6-benzylaminopurine to catalase: multiple spectroscopic methods combined with molecular docking study, Spectrochim. Acta A 123 (2014) 327–335.
[31] D. Majumder, A. Das, C. Saha, Catalase inhibition an anti cancer property of flavonoids: a kinetic and structural evaluation, Int. J. Biol. Macromol. 104 ((2017) 929–935.
[32] B. Koohshekan, A. Divsalar, M. Saiedifar, A.A. Saboury, B. Ghalandari, A. Gholamian, A. Seyedarabi, Protective effects of aspirin on the function of bovine liver catalase: a spectroscopy and molecular docking study, J. Mol. Liq. 218 (2016) 8–15.
[33] L. Yang, D. Huo, C. Hou, M. Yang, H. Fa, X. Luo, Interaction of monosulfonate tetraphenyl porphyrin (H2TPPS1) with plant-esterase: determination of the binding mechanism by spectroscopic methods, Spectrochim. Acta A 78 (2011) 1349–1355.
[34] R. Yekta, G. Dehghan, S. Rashtbari, R. Ghadari, A. Moosavi-Movahedi, The inhibitory effect of farnesiferol C against catalase; kinetics, interaction mechanism and molecular docking simulation, Int. J. Biol. Macromol. 113 (2018) 1258–1265.
[35] Y. Teng, L. Zou, M. Huang, W. Zong, Molecular interaction of 2-mercaptobenzimidazole with catalase reveals a potentially toxic mechanism of the inhibitor, J. Photochem. Photobiol. B 141 (2014) 241–246.
[36] M. van de Weert, L. Stella, Fluorescence quenching and ligand binding: a critical discussion of a popular methodology, J. Mol. Struct. 998 (2011) 144–150.
[37] R. Yekta, G. Dehghan, S. Rashtbari, N. Sheibani, A. Moosavi-Movahedi, Activation of catalase by pioglitazone: multiple spectroscopic methods combined with molecular docking studies, J. Mol. Recognit. 30 (2017) 1–11.
[38] J.R. Lakowicz, Principles of Fluorescence Spectroscopy, Springer, New York, 2006.
[39] S. Rashtbari, G. Dehghan, R. Yekta, A. Jouyban, M. Iranshahi, Effects of resveratrol on the structure and catalytic function of bovine liver catalase (BLC): spectroscopic and theoretical studies, Adv. Pharm. Bull. 7 (2017) 349–357.
[40] M. Xu, Z. Cui, L. Zhao, S. Hu, W. Zong, R. Liu, Characterizing the binding interactions of PFOA and PFOS with catalase at the molecular level, Chemosphere 203 (2018) 360–367.
[41] X. Wei, Z. Ge, Effect of graphene oxide on conformation and activity of catalase, Carbon 60 (2013) 401–409.
[42] M.R. Murthy, T.J. Reid, A. Sicignano, N. Tanaka, M. Rossman, Structure of beef liver catalase, J. Mol. Biol. 152 (1981) 465–499.